

**Paper No.
MC34**



Control of corrosion and activation of the Mo doped Mn ferrite based electrode with respect to enhanced power generation in a Microbial Fuel Cell

B.R.Sreelekshmy

Department of Biotechnology, University of Kerala, Thiruvananthapuram, Kerala, India
b.rsreelekshmi@gmail.com

Chinnu M. Lal, Suma M.S., S.M.A. Shibli

Department of Chemistry, University of Kerala, Thiruvananthapuram, Kerala, India

ABSTRACT

Iron oxide based magnetic nanoparticles have attracted enormous attention due to their biocompatibility and low toxicity and are being widely used in biological applications like controlled drug delivery, cell separation, magnetic resonance imaging and localized hyperthermia therapy of cancer. Among these, manganese ferrites are important members of ferrite family with a variety of application in science and engineering. This study reports the effects of Mo doping on Mn ferrite (Mo-MnF) to improve conductivity, active site accessibility and electrochemical stability for the electrode in Microbial fuel cell (MFC). As a promising material, Mo-MnF [$Mn_{(1-x)} Mo_x Fe_2O_4$ ($x = 0.0, 0.3, 0.5, 0.7, 1$)] nanoparticles were prepared by thermal decomposition method and electrode prepared by electroless coating of Ni-P with Mo-MnF. The material structure and crystalline size of the prepared samples were analysed with XRD. The morphological characterization, surface structure, and electrochemical properties were studied using SEM, CSLM, AFM FT-IR, EIS, CV and polarization studies.

NIGIS * CORCON 2017 * 17-20 September * Mumbai, India

Copyright 2017 by NIGIS. The material presented and the views expressed in this paper are solely those of the author(s) and do not necessarily by NIGIS.

The results confirmed the formation of pure and cubic spinel structure, with the average grain size of 20-15 nm. SEM images clearly showed the agglomerated nature of nanoparticles. There was a significant increase in the stability of the developed electrodes, corrosion resistance and electrocatalytic activity towards the oxidation of microbial fermentation. MFC was constructed with these developed electrodes and run for about 3 months under aerobic condition and obtained a cell potential of about 0.78V and current density of about 0.4mA/cm² on 7th day of operation and remained stable for 3200hrs. This study put forth a novel corrosion resistive composite with future potential for a biocompatible and cost effective electrode that is easy to synthesize.

Keywords: Mn ferrite; Mo doping; Corrosion; Microbial fuel cell

INTRODUCTION

Energy is an unavoidable need in the present scenario. The existence of a society totally depends upon energy, as its application is widely distributed in various fields. Even if, the present world is depending on fossil fuels, it is under the threat of depletion and the pollution caused by fossil fuel is another problem. But as a solution many alternative forms of energy have been adopted. Thus the development of energy from renewable energy sources is a vital need. Microbial fuel cell (MFC) is a novel and unique invention capable of solving problems which are tumbling from crisis to crisis. i.e; energy generation and its demand.

MFC is based on the electrochemical catalyst reaction realized by exoelectrogenic bacteria (EB) on the anode to produce electricity. So the adhesion of bacteria to anode surface can enrich the current generation. The performance of fuel cell strongly depends on the efficacy of the electrode. Therefore, electrode design is a key factor for an efficient and inexpensive MFC fabrication. An electrode should have characteristics such as large active surface area, physical and electrochemical stability, low cost, ease of use and good electrical conductivity. Generally biocompatible conductive carbon paper/ cloth, graphite, iron oxides and stainless steel are utilized as anode in MFC's. However these materials lack electrochemical activity and are very expensive too. There for development of highy corrosion resistant and cost effective electrode is inevitable. Among the studied transition metals, nickel and its alloy exhibit good corrosion and wear resistance in aggressive environment. Incorporation of transition metals with in Ni-P electroless coating can greatly improve their catalytic activity and efficiency of MFC. Among the transition metal oxides nanoparticles, manganese ferrites (Mn Fe₂O₄) exhibits electrocapacitive behaviour as good as platinum (Pt). But semiconducting nature of Mn Fe₂O₄ reduces its electrochemical activity. The corrosion resistance and electrocatalytic activity can be further enhance by doping with suitable metals.

Based on the above facts, our aim is to synthesis and tuning of various concentration of Molybdenum doped Mn Fe₂O₄ [Mn_(1-x) Mo_xFe₂O₄ (x = 0.0, 0.3, 0.5, 0.7, 1)] on the basis of its stability, crystalline nature, biocompatibility and electrochemical activity. Then the superior oxides were used as a catalyst and coated on to the mild steel substrate using Ni-P electroless plating and its catalytic activity and corrosion resistance property is studied at different concentration. The developed coating should exhibit high stability and tolerance. The influence of structure, morphology and phase of the oxides catalysts over the MFC performances has to be detailed and compared with the Mn Fe₂O₄ as reported earlier. The study should account for the stability of composite for application in various other fields.

NIGIS * CORCON 2017 * 17-20 September * Mumbai, India

Copyright 2017 by NIGIS. The material presented and the views expressed in this paper are solely those of the author(s) and do not necessarily by NIGIS.

EXPERIMENTAL PROCEDURE

PREPARATION OF MO DOPING ON $MnFe_2O_4$ AND CHARACTERIZATION

Various compositions of Mo doped $MnFe_2O_4$ were prepared by thermal decomposition method based on the formula $Mn_{(1-x)} Mo_x Fe_2O_4$ ($x = 0, 0.3, 0.5, 0.7, 1$). Required amount of $FeCl_3$, $MnCl_2 \cdot 4H_2O$ and MoO_3 was dissolved in 150mL aqueous solution and it was then added with 35ml ammonia solution with vigorous stirring. It was kept at room temperature for 1h. The mixture was placed in a china dish followed by heating at $180^\circ C$ in an autoclave for 12-16 h. The powder thus obtained was cooled and was finely ground using motor and pestle. The precipitate was collected through centrifugations after washing with distilled water and ethanol. The precipitate obtained was kept in a vacuum oven for 8 h by heating at $90^\circ C$. This method was repeated for the rest.

The prepared oxide is characterized by XRD, UV- Visible spectroscopy, FTIR, SEM, Raman spectroscopy. The biocompatibility of the prepared oxide was prepared by crystal violet biofilm formation assay test.

MILD STEEL

In the present study, mild steel having the composition: Fe – 99.152%, Mn – 0.34%, P – 0.34%, C – 0.09%, Si – 0.049%, Mo– 0.029% was used as the substrate for anode

PREPARATION OF NI- P COATINGS AND CORROSION CHARACTERIZATION

Mild steel strips having dimensions of 3 cm x 2 cm x 1 mm were selected and they were polished to mirror finish manually. Steels were washed with distilled water followed by treatment with 5% NaOH solution for 5 min Rinsed again with water and etched in 3% HCl for 5 min (ASTM B 656). The substrate was sensitized by immersing in a solution containing $SnCl_2$ (10g/L) (Sigma Aldrich, assay 99%) in 37% HCl (40mL/L). The sensitized substrate was immersed in $PdCl_2$ (1g) and HCl 10 mL solution for 0.5 – 2 min. This activated mild steel was taken for the coating process. The bath was prepared using the composition: 30 g/L nickel sulphate (Sigma Aldrich, assay 99%) and 25 g/L succinic acid (Sigma Aldrich, assay 99%). Its pH and temperature was maintained at 4.5 and $80-85^\circ C$. After attaining $60^\circ C$, 25 g/L sodium hypophosphite (Sigma Aldrich, assay 99%) was added and surface activated specimen was introduced into the bath by means of a connecting wire. Different amounts of Fe_2TiO_5 composite were added into the bath and stirred constantly during the coating process to get Fe_2TiO_5 composite incorporated Ni-P coating plates. After 2hr of coating process, substrate removed from bath and rinsed with warm distilled water and the substrate after drying, wrapped and kept for testing the performance.

Tafel extrapolation polarization resistance (R_p) are polarization techniques used to determine the corrosion rate of optimized sample. It was carried out under Potentiodynamic condition of 250 mv above the potential equilibrium. Parameters like E_{corr} corrosion potential, I_{corr} corrosion current, tafel constants β_a (anodic coefficients) and β_c (cathodic coefficient) and polarization resistance R_p for electrode reactions can be determined.

CONSTRUCTION OF MFC AND EVALUATION

A dual chambered MFC was set up using mild steel modified Ni –P incorporated Mo doped $MnFe_2O_4$ (1.56 cm diameter and 1mm thickness). Two glass bottles of 100 mL volume served as anode and cathode chambers.

NIGIS * CORCON 2017 * 17-20 September * Mumbai, India

Copyright 2017 by NIGIS. The material presented and the views expressed in this paper are solely those of the author(s) and do not necessarily by NIGIS.

The anode chamber was inoculated with mixed culture which was grown on PBS based cultivation medium [$K_2HPO_4 \cdot 3H_2O$ (3.4g/L), KH_2PO_4 (4.4g/L)] which contains PBS based glucose (g/L), CH_3COONa (1.6g/L), NH_4Cl (1.5g/L), $MgCl_2 \cdot 6H_2O$ (0.1g/L), trace mineral metal solution (10mL/L). The cathode chamber was kept at anaerobic condition and was constituted with a PBS solution ($K_2HPO_4 \cdot 3H_2O$ (3.4g/L), 4.4g/L KH_2PO_4 , 0.1M, P^H 7.5) containing potassium ferricyanide (16.64g/L) and the entire set up was kept at room temperature. From polarization curves the maximum power density of MFC was determined.

RESULTS

CHARACTERIZATION OF THE PREPARED $Mn_{(1-x)} Mo_x Fe_2O_4$ NANOPARTICLES

The crystalline nature and phase characterization of as synthesised $Mn_{(1-x)} Mo_x Fe_2O_4$ samples where $x = 0, 0.3, 0.5, 0.7, 1$ were analysed by powder XRD (PXRD) and is shown in figure. 3.1.

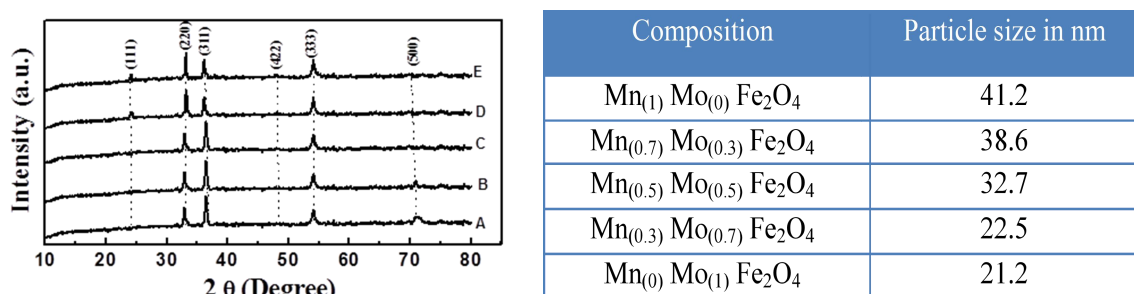


Fig 3.1 Phase identity of $MnFe_2O_4$ and Mo doped $MnFe_2O_4$ nanoparticles and Variation of particle size in nm

All the peaks of all the samples show the characteristic reflection of spinel cubic crystal structure of ferrite even in the heavy doped nanoparticles. This spinel lattice indicating their single phase structure with no traces of other impurity (eg. Fe_2O_3 , Mn etc.). The peak could be indexed as (111), (220), (311) and (333) which were observed at $2\theta = 23.65^\circ$, 32.05° , 35.73° and 54.58° . It can be seen that, the sites and intensity of the diffraction peaks are consistent with the standard pattern for JCPDS Card No. 89-4319. Broad peaks of the sample revealed the ultrafine nature of the nanoparticles. From the figure it was clear that as Mo content increases the reflection peak slightly shift to lower angle. An intense peak at the plane (311) was considered as a measure of crystallinity. The average crystalline size of the samples were calculated by measuring full width at half maximum (FWHM) for each samples with the help of Debye- Scherrer formula, [1]. The calculated values of crystalline size are summarized in table. From the table it has been observed that the crystalline size is decreased from 41.2 nm to 21.0 nm with increase in Mo content from $x=0$ to $x=1$, which may attribute to the difference in cationic radii. This decrease in the value of crystalline size may be attributed to the quantum confinement in nanoparticles, due to replacement of Mn which have higher ionic radii (0.91 \AA) compared to Mo ions (0.83 \AA). Since lattice parameter is related to particle size and d- spacing decrease in lattice constant was expected. A linear decrease in lattice spacing indicates that the Mn ions are replacing the Mo ions in Mn ferrite matrix. This explains the decrease of lattice constant with Mo doping and also confirms that Mo is occupied in the lattice of spinel ferrites [2].

The effect of doping level in Fourier transform infrared spectroscopy (FT-IR) transmission spectra in the region 4000-400 cm^{-1} is explained in the figure 3.2.

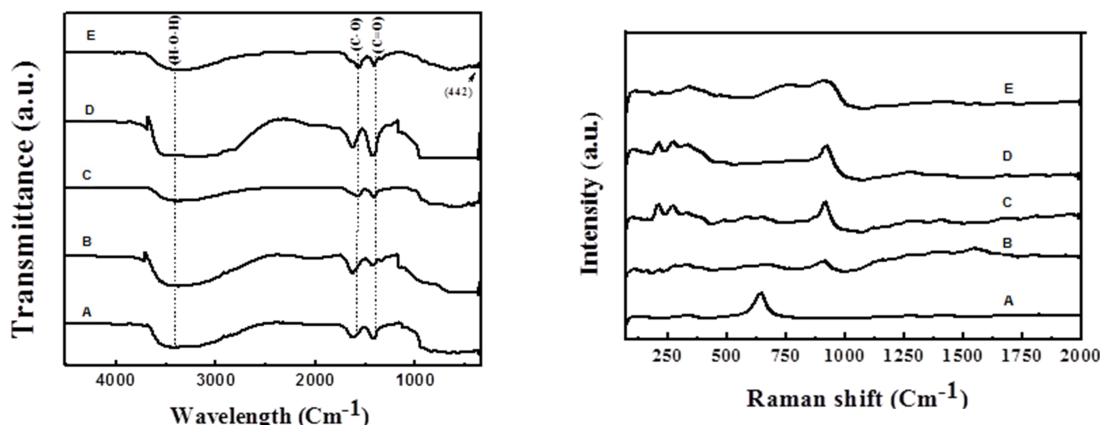


Fig. 3.2 FTIR spectra and Raman spectra of the prepared $\text{Mn}_{(1-x)}\text{Mo}_x\text{Fe}_2\text{O}_4$ nanoparticles where (A) $x = 0$ (B) $x = 0.3$ (C) $x = 0.5$ (D) $x = 0.7$ (E) $x = 1$

IR spectra data of all samples prepared by this methods are found to show two absorption bands at 584 cm^{-1} and 442 cm^{-1} are the vibration of (Fe-O) which are indication of formation of spinel ferrite structure which are in agreement with the reported value (0). In addition all the samples show absorption band around 3435.22 cm^{-1} which corresponds to stretching vibration of hydroxyl functional group of adsorbed water in the sample. The adsorption band at 1721 cm^{-1} corresponds to stretching vibration of carbonyl group (C-O) [3].

The Raman spectra of MnFe_2O_4 nano crystalline samples have hardly visible doublet structure. Doublet modes at 590-670 cm^{-1} is observed for MnFe_2O_4 . Raman spectra of MnFe_2O_4 and Mo doped MnFe_2O_4 prepared by thermal decomposition method at 180°C is given in the figure 3.2. The modes at 590- 670 cm^{-1} correspond to A_g symmetry and a mode observed in the range of 590-670 cm^{-1} for MnFe_2O_4 can be assigned to tetrahedral Mn^{2+} stretching. Band observed at 484 cm^{-1} can be assigned to octahedral Fe^{3+} vibration at the octahedral site. The other three modes obtained at about 214, 380 and 484 cm^{-1} for MnFe_2O_4 belongs to F_{2g} symmetry type.

The effect of doping of Mo on Manganese ferrites nanoparticles on bacterial growth and biofilm formation by *P.putida* was measured using crystal violet biofilm formation assay and shown in the figure 3.3 (a) and (b).

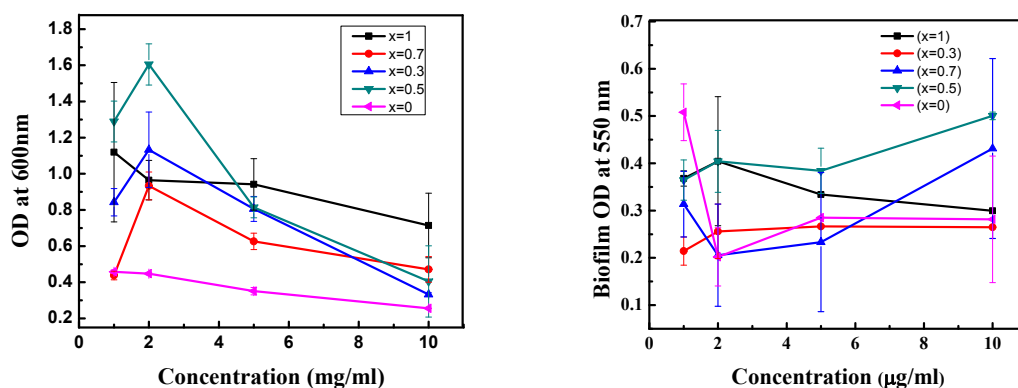


Fig.3.3 (a) Effect of $\text{Mn}_{(1-x)}\text{Mo}_x\text{Fe}_2\text{O}_4$ on bacterial growth and (b) biofilm formation by *P.putida* after 16 hrs.

NIGIS * CORCON 2017 * 17-20 September * Mumbai, India

Copyright 2017 by NIGIS. The material presented and the views expressed in this paper are solely those of the author(s) and do not necessarily by NIGIS.

From the figure 3.3 (a) and (b), it was clear that addition of all $Mn_{(1-x)} Mo_x Fe_2O_4$ samples did not show any toxicity even at the concentration of 10 mg/ml. In fact there was a significant increase in biofilm and biomass with $Mn_{(1-x)} Mo_x Fe_2O_4$ ($x = 0.3, 0.5, 0.7$) compared with $Mn_{(1-x)} Mo_x Fe_2O_4$ ($x = 0$). There was also a 2 fold increase in the cell density of population exposed to $Mn_{(1-x)} Mo_x Fe_2O_4$ ($x = 0.3, 0.5, 0.7$) compared with $Mn_{(1-x)} Mo_x Fe_2O_4$ ($x = 0$) and without nanoparticles. That is, addition of $Mn_{(1-x)} Mo_x Fe_2O_4$ can stimulate the bacterial growth and biofilm formation. Whereas $Mn_{(1-x)} Mo_x Fe_2O_4$ with $x = 0.5$ showed more activity. The surface morphology and micro structures of the samples were revealed by SEM analysis. Fig: 3.5(a) shows the presence of $Mn_{(1-x)} Mo_x Fe_2O_4$ with $x = 0.5$.

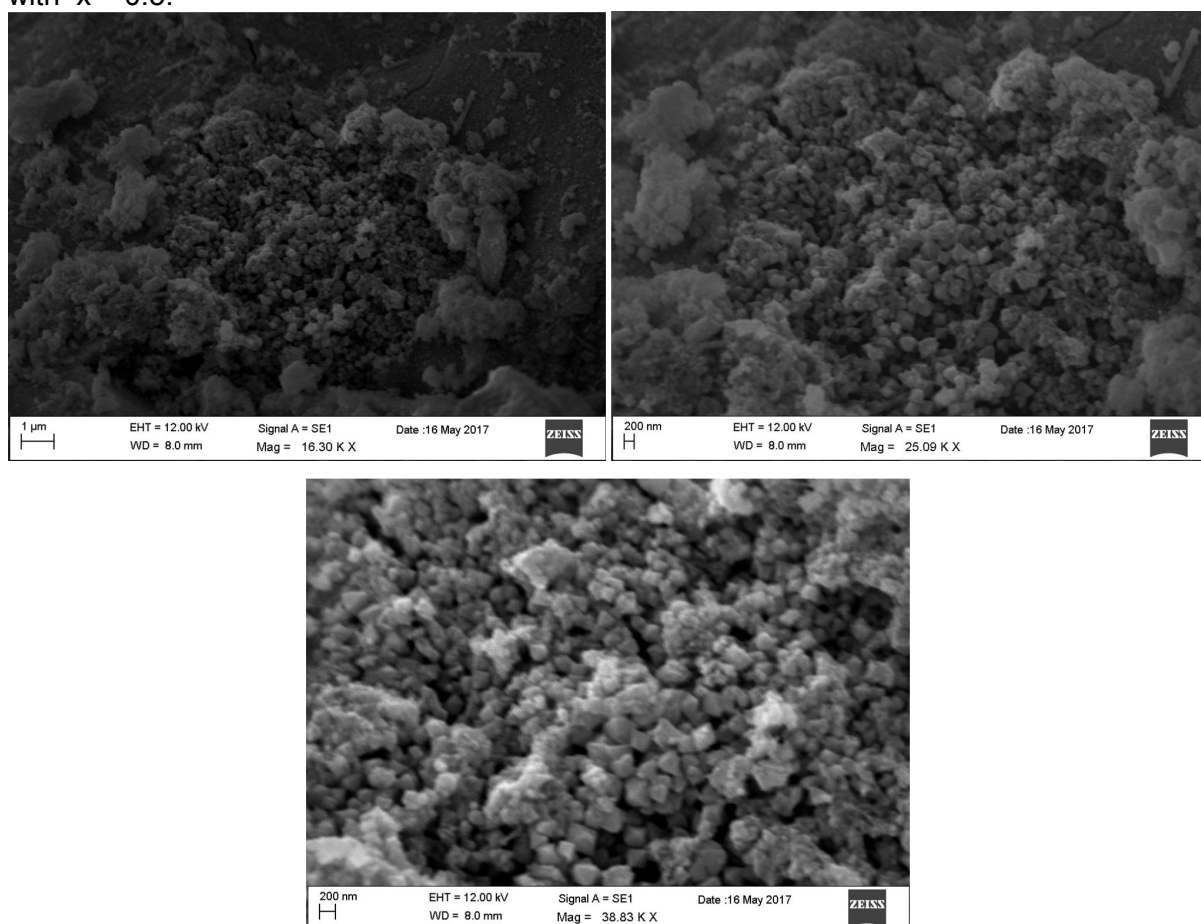


Fig. 3.4 (a) SEM images of $Mn_{(1-x)} Mo_x Fe_2O_4$ where $x = 0.5$ at 16, 000X (A), 25,000 X (B) and 35,000 X (C) respectively.

The surface features of $Mn_{(1-x)} Mo_x Fe_2O_4$ ($x = 0.5$) was clear from SEM micrographs 3.4 (a). It is cleared that the microstructure of the grains of the sample is ultra small and homogenous with cuboid in shape and agglomerated. This agglomeration may be due to the presence of magnetic interactions.

A

B

NIGIS * CORCON 2017 * 17-20 September * Mumbai, India

Copyright 2017 by NIGIS. The material presented and the views expressed in this paper are solely those of the author(s) and do not necessarily by NIGIS.

Characterization of $Mn_{(1-x)} Mo_x Fe_2O_4$ ($x = 0.5$) incorporated Ni-P coatings

The successful incorporation of $Mn_{(1-x)} Mo_x Fe_2O_4$ ($x = 0.5$) and ($x = 0$) nanoparticles and its crystalline structure can be analysed by XRD characterization. XRD pattern of $Mn_{(1-x)} Mo_x Fe_2O_4$ ($x = 0.5$) (1g/l, 2g/l and 5g/l) incorporated electroless Ni-P coating on mild steel substrate was shown in the figure 3.5 (A, B and C).

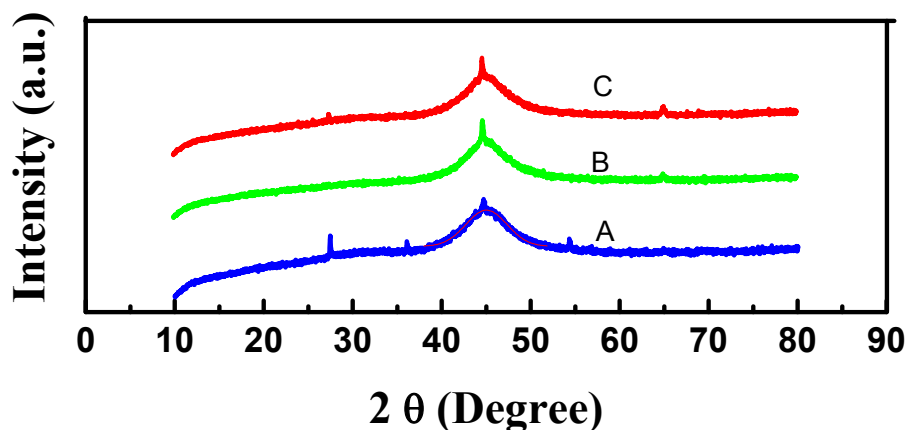
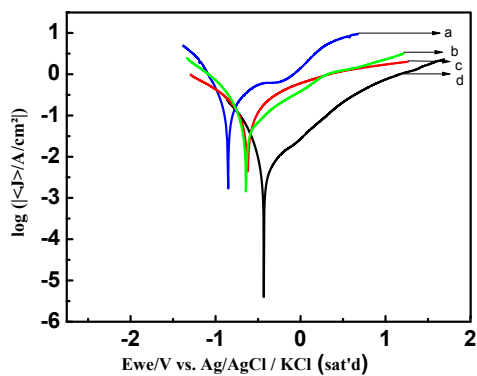


Fig. 3.5 XRD pattern of $Mn_{(1-x)} Mo_x Fe_2O_4$ ($x = 0.5$) incorporated electroless Ni-P coating (A) 2g/l, (B) 1g/l, and (C) 5g/l

From the figure it was clear that, a sharp peak at $2\theta = 36.45^\circ$ and 26.26° of sample A which confirms the presence of $Mn_{0.5} Mo_{0.5} Fe_2O_4$ phases that shows the successful incorporated of nanoparticles into the Ni-P coating. Whereas peak at $2\theta = 45.45^\circ$ corresponds to amorphous nature of coated Ni-P. Sample B (1g/l) and sample C (5g/l) shows a little incorporation. This may be due to the insufficient amount of nanoparticles in the bath for successful incorporation and in case of bath containing 5g/l of nanoparticles result in agglomeration of nanoparticles and increase in grain size and thus failure of incorporation. The electrochemical properties of these coated electrodes were further investigated by tafel polarization.

The electrochemical evaluation of various concentration $Mn_{(1-x)} Mo_x Fe_2O_4$ ($x = 0.5$) nanoparticles incorporated Ni-P coatings were shown in the figure 3.6.



Samples	E_{corr} (mV vs. Ref)	I_{corr} ($\mu\text{A}/\text{cm}^2$)	β_c (mV)	β_a (mV)	C_R (mmpy)
MnFe_2O_4	-638.720	33 643.176	194.9	459.5	110.08
$\text{Mn}_{(0.5)}\text{Mo}_{(0.5)}\text{Fe}_2\text{O}_4$ (1g/L)	-627.098	45 390.379	275.6	319.6	148.517
$\text{Mn}_{(0.5)}\text{Mo}_{(0.5)}\text{Fe}_2\text{O}_4$ (2g/L)	-428.468	909.162	60.9	109.1	2.974 78
$\text{Mn}_{(0.5)}\text{Mo}_{(0.5)}\text{Fe}_2\text{O}_4$ (5g/L)	-689.142	25 130.787	74.0	121.1	82.227 9

Fig 3.6 Tafel polarization curve and table showing the tafel parameters of various concentrations of $\text{Mn}_{(1-x)}\text{Mo}_x\text{Fe}_2\text{O}_4$ ($x = 0.5$) nanoparticles incorporated Ni- P coating (a) MnFe_2O_4 , (b) 1g/l, (c) 5g/l, (d) 2g/l

From the figure 3.8 and table it was clear that all the $\text{Mn}_{(1-x)}\text{Mo}_x\text{Fe}_2\text{O}_4$ ($x = 0.5$) samples show better electrochemical activity than compared to MnFe_2O_4 . It gives information about the corrosion kinetic process and only method to reveal anodic and cathodic contributions. The coating co deposited with $\text{Mn}_{(1-x)}\text{Mo}_x\text{Fe}_2\text{O}_4$ ($x = 0.5$) with bath containing 2g/l shows the most protective coating on the basis of low I_{corr} and high polarization resistance. It means that $\text{Mn}_{(1-x)}\text{Mo}_x\text{Fe}_2\text{O}_4$ ($x = 0.5$) (2g/l) coating is more stable and less soluble compared to other coatings. Corrosion potential and corrosion current density was obtained by the intersection of the extrapolation of anodic and cathodic tafel curves. From the table 3.2 it was clear that, as concentration of nanoparticles in the bath composition increased, incorporation also increased and thus formed a protective layer up to 2g/l which has blocked the further corrosion. From the polarization curves, protection efficiency P_i (%) index can be calculated. Where I_{corr} and I_{corr}^0 indicate the corrosion current density of $\text{Mn}_{(1-x)}\text{Mo}_x\text{Fe}_2\text{O}_4$ ($x = 0.5$) and MnFe_2O_4 respectively. $\text{Mn}_{(1-x)}\text{Mo}_x\text{Fe}_2\text{O}_4$ ($x = 0.5$) coated electrode with 2g/l bath composition shows the maximum protection efficiency P_i (%) index of 78% caused by lowest current density of $9.09 \times 10^2 \mu\text{A}/\text{cm}^2$ than that compared with the MnFe_2O_4 . Thus $\text{Mn}_{(1-x)}\text{Mo}_x\text{Fe}_2\text{O}_4$ ($x = 0.5$) 2g/l bath composition shows maximum activity and corrosion resistance and thus suitable for MFC construction.

3.4 Construction and evaluation of MFC

Double chambered MFC was fabricated with optimized concentration of $\text{Mn}_{(1-x)}\text{Mo}_x\text{Fe}_2\text{O}_4$ nanoparticle coated electrode. Anodic and cathodic potential were measured individually against calomel electrode and cell potential were calculated. From this data power density and current density were calculated and compared with that of MFC with MnFe_2O_4 . The anodic and cathodic electrode potential curves verses reference electrode of constructed MFC were measured and plotted in figure 3.7.

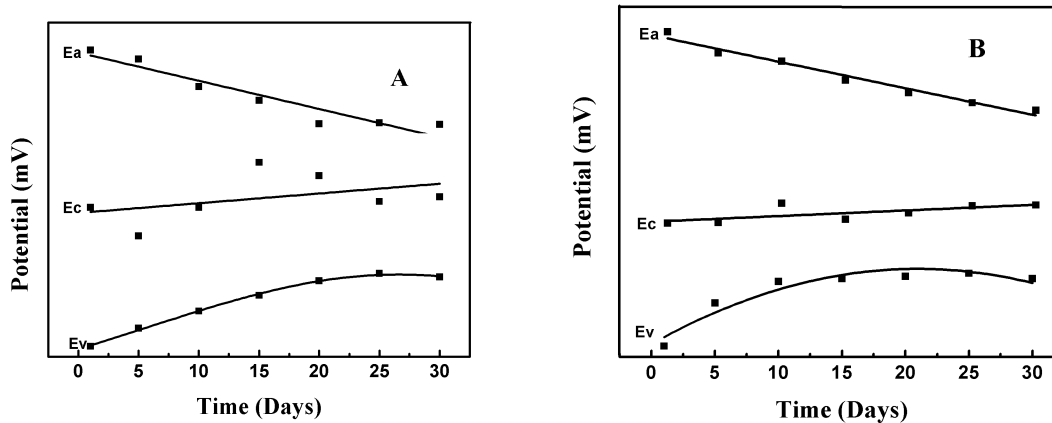


Fig. 3.7 The anodic (Ea), cathodic (Ec) and cell (Ev) potential curves verses reference electrode of constructed MFC of (A) Mn Fe₂O₄ and (B) Mn_(1-x) Mo_x Fe₂O₄ (x = 0.5)

A gap in mV between the curves equals the cell voltage (Ev). Anodic and cathodic potential curves make it possible to determine the performance of each electrode reaction separately, whereas cell potential gives the performance of entire MFC. From the figure Mn_(1-x) Mo_x Fe₂O₄ (x = 0.5) (B) coated electrode showed a maximum anodic potential of -585 mV and cell voltage of 890 mV, which is 2 fold higher than electrode coated with Mn Fe₂O₄. This increase in cell potential may be due to high interaction of anode with the substrate and bacteria present in the anolyte. The electrode which limits the performance will result in curve with steep slope which is evident from the figure 3.7 (A). A fast drop in anodic potential can also be seen from the figure.

Power density verses current density curve of the MFC constructed with MnFe₂O₄ and Mn_(1-x) Mo_x Fe₂O₄ (x = 0.5) incorporated through Ni- P coating was shown in the figure 3.8.

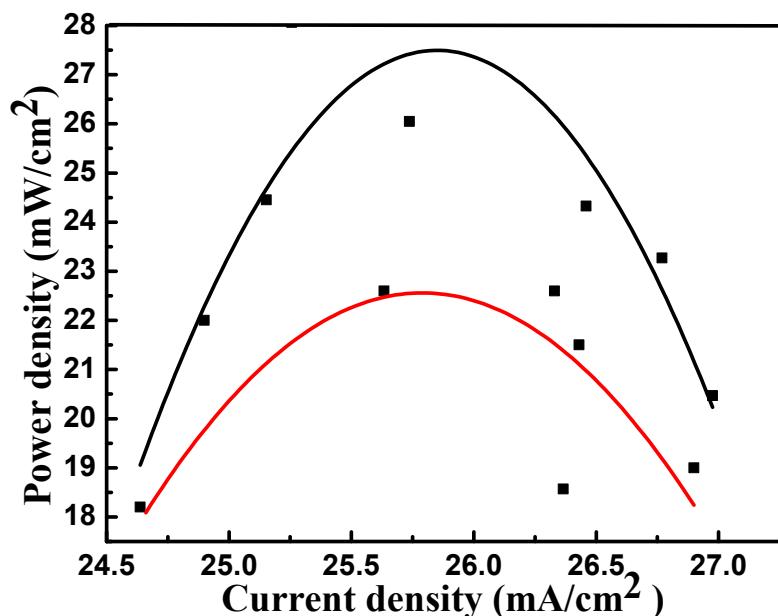


Fig. 3.8. Power density curve of MFC constructed with MnFe₂O₄ (Red) and Mn_(1-x) Mo_x Fe₂O₄ (x = 0.5) (Black)

Power density curve of MFC using pretreated sugarcane bagasse as substrate for mixed culture bacteria. From the figure it was clear that, the MFC with $Mn_{(1-x)} Mo_x Fe_2O_4$ ($x = 0.5$) modified mild steel anode obtained a maximum power density of 27.8 mW/cm^2 and current density of 39.4 mA/cm^2 which is 2 fold more than $MnFe_2O_4$ modified electrode. From these results it can be concluded that, anode modification using Mo doped $MnFe_2O_4$ was found to increase the hydrophobicity, bioactivity which facilitated the bacterial interaction with anode and thus increased the power and current output.

CONCLUSIONS

ACKNOWLEDGMENTS

The authors are grateful to the Prof. and Head, Department of Chemistry, University of Kerala for providing facilities to carry out this work.

REFERENCES

- [1] Kamala Bharathi K, Markandeyulu G and Ramana C V. Structural, magnetic, electrical and magnetoelectric properties of Sm- and Ho substituted nickel ferrites. *Journal of Physical Chemistry C*, 115:554-560. [http:// dx.doi.org/10.1021/jp1060864](http://dx.doi.org/10.1021/jp1060864) (2011)
- [2] Characterization of nanometric Mn ferrite through different methods *Nanotechnology* 19(2008) 065603(6pp)
- [3] Structural, infrared and elastic properties of lithium ferrite. *India Journal of Pure and Applied Physics*. Vol45, July 2007, pp.596-608
- [4] Ivanov, Ivan ; et.al(2010). "Recent advances in enzymatic fuel cells: Experiments and Modelling". *Energies*.3(4).
- [5] Lu, Z.; Chang, D.; Ma, J.; Huang, G.; Cai, L.; Zhang, L.(2015). "Behaviour of metal ions in bioelectrochemical systems: A review". *Journal of Power Sources*. 275: 243-260. doi:10.1016/j.jpowsour.2014.10.168.
- [6] Bond, D.R.; Lovely, D.R electricity production by *Geobacter sulfereducens* attached to electrodes. *Appl. Environ. Microbiol.*2003,69.1548-1555.
- [7] Sankara Narayanan T S N, Bhaskaran I, Krishnadevi K, Prathibhan S. Deposition of electroless Ni-P graded coatings and evolution of their corrosion resistance. *Surface coating technology*,2006; 200. 3438-3445
- [8] N. Ozer and F. Tepehen, Optical and electrochemical characteristics of Sol- gel deposited iron oxide films. *Solar energy materials and solar cells*, 56:p.141-152(1999)
- [9] Chen L Y, Dai H, Shen Y M and Bai J F. Size controlled synthesis and magnetic properties of $NiFe_2O_4$ hollow nanospheres via a gel assistant hydrothermal route. *Journal of Alloys and Compounds*. 491: L 33- L-38(2010)
- [10] S.Komarneni, E.Fregeau, E.Breval, and R.Roy, "Hydrothermal preparation of ultrafine Ferrites and their sintering". *J. Am. Ceram. Soc.*,71(1) C-26-C 289(1998)
- [11] M. Gurumoorthy, K. Parasuraman, M. Anbarasn and K.Balamurugan. *International Research Journal of Nanoscience and Technology*. Synthesis and characterization of $MnFe_2O_4$ nanoparticles by hydrothermal methods.vol.5 (4-6), 101-106, April- June 2015
- [12] Zheng Han, Da Li, Xianguo Liu, Dianyu Geng, JiLi and Zhidongzhang, Microwave absorption properties of Fe(Mn)/ ferrite nano capsules, *Journal of Physics D; Applied Physics*. 42(2009) 055008
- [13] Vikas J. Pisserlekar, Effect on properties of $ZnFe_2O_4$ ferrites on doping with manganese ions. *International Journal of Science and Research*, vol 5, issue 2, February 2016.

NIGIS * CORCON 2017 * 17-20 September * Mumbai, India

Copyright 2017 by NIGIS. The material presented and the views expressed in this paper are solely those of the author(s) and do not necessarily by NIGIS.